

Cite this: *Polym. Chem.*, 2026, **17**, 971

Superionic conduction in solid polymer electrolytes – decoupling ion transport from segmental relaxation

Mengying Yang ^a and Thomas H. Epps, III ^{*a,b,c}

Solvent-free, solid polymer electrolytes (SPEs) are promising candidates for next-generation, electrochemical energy storage systems due to their potential to enhance safety and performance, enable flexible device architectures, and streamline manufacturing processes. Conventional SPEs suffer from limited ionic conductivity due to the strong coupling between ion transport and (generally slow) polymer segmental relaxation. The realization of superionic conduction in SPEs, in which ions move faster than the structural relaxation of the polymers, requires a shift in design principles to promote this type of decoupled ion motion. In this perspective, we discuss how polymer architecture, ion–ion correlations, and ion–polymer interactions can unlock superionic behavior. We highlight several key design features, such as crystallinity, bulky side groups, high molecular weight, and percolating ionic aggregation, with a focus on creating low-barrier transport pathways in various polymer systems. We also demonstrate opportunities to combine polymer chemistry and data science through high-throughput and automated screening approaches to reveal how phase behavior, ion dynamics, and ionic interactions govern transport, thereby potentially enabling data-driven discovery of superionic polymer electrolyte materials.

Received 12th November 2025,
Accepted 8th February 2026

DOI: 10.1039/d5py01070e

rsc.li/polymers

Introduction

Lithium-ion batteries (LiBs) are a key technology for powering portable electronics, electric vehicles, and grid-scale storage systems due to their high energy densities, low self-discharge rates, and minimal memory effects.^{1–7} LiBs consist of one or more connected electrochemical cells,⁸ and each cell contains a cathode and an anode separated by an electrolyte-separator system. Conventional electrolytes typically comprise a lithium salt (*e.g.*, LiPF₆) and stabilizing additives dissolved in a mixture of carbonate-based liquid solvents (*e.g.*, ethylene carbonate and dimethyl carbonate).^{2,9} Although this class of electrolytes offers high ionic conductivities at room temperature ($\sim 10^{-2}$ S cm⁻¹),^{2,10} it suffers from low lithium transference numbers (*i.e.*, fraction of current carried by Li⁺, t_{Li^+} , <0.5). The low t_{Li^+} s result from a transport mismatch between Li⁺ and the anion. Lithium ions are surrounded by bulky solvation shells, which significantly slow their movement in comparison to the anions.¹¹ This imbalance can

lead to concentration gradients during battery operation, eventually resulting in salt depletion at one electrode and precipitation at the other.¹² Over time, this effect can cause battery failure, and in severe cases, even catastrophic explosions.¹³ Additionally, the low t_{Li^+} s limit the current density that the battery can support, thereby restricting charge and discharge rates.¹⁴

To meet the demand for higher-performing LiBs, new electrolyte systems must be developed to address the above-mentioned safety and performance challenges. Solid polymer electrolytes (SPEs) are one attractive option due to their versatility and processability.¹⁵ Conventional SPEs, typically flexible polymers with glass transition temperatures (T_g s) below 25 °C, rely on segmental mobility to create a dynamic environment for ion transport.^{16,17} The chain flexibility of these SPEs promotes the formation of closely packed structures with limited free volume between polymer chains.¹⁸ As a result, ions move only when the polymer matrix undergoes local movement, *i.e.*, polymer segmental motion,^{19,20} which is inherently slow and becomes even slower with increasing ion concentration, as more ions are coordinated to the polymer – ultimately resulting in reduced conductivities.²¹

To overcome this limitation, one can consider superionic transport, in which ions move faster than the polymer matrix relaxes by decoupling of ion motion from polymer segmental dynamics. Decoupled ion transport typically can be identified through a modified Walden plot analysis, in which molar con-

^aDepartment of Materials Science & Engineering, University of Delaware, Newark, DE 19716, USA^bDepartment of Chemical & Biomolecular Engineering, University of Delaware, Newark, DE 19716, USA^cCenter for Research in Soft matter & Polymers (CRISP), University of Delaware, Newark, DE 19716, USA

ductivity is plotted against the inverse of segmental relaxation time,¹⁸ as shown in Fig. 1. τ is determined from the frequency at the crossover of the storage and loss moduli at high frequencies.¹⁸ A solid line with a slope of 1 represents the ideal Walden line, which was established using reference systems of dilute aqueous solutions of salts (e.g., KCl, LiCl, LiClO₄),²² wherein the ionic interaction is much weaker than thermal energy.²² The ideal Walden line divides the Walden plot into a superionic region (above the line) and a subionic region (below the line).²² Systems that fall on the Walden line indicate complete dissociation of ion pairs and that ion motion is closely coupled with the segmental motion,^{18,22} whereas systems in the subionic region typically have low free ion concentrations.²² Superionic electrolytes have ions moving faster than the structural relaxation of the polymers.²² The degree of decoupling, ϵ , can be calculated as $1 - \alpha$, in which α is the modified Walden plot slope. This parameter quantifies the extent to which ionic conductivity becomes decoupled from segmental relaxation in the vicinity of T_g .²³

Another approach to characterizing ionic motion that is independent of segmental relaxation is to examine Arrhenius-type temperature-dependent behavior,^{24–27} that is, the conductivity follows the Arrhenius equation [eqn (1)],²⁸

$$\sigma = \sigma_0 \exp\left(\frac{-E_a}{RT}\right) \quad (1)$$

in which σ_0 is the ionic conductivity at infinitely high temperature,^{4,29} E_a is the pseudo activation energy associated with ion hopping, R is the ideal gas constant, and T is the absolute temperature in Kelvin.

To facilitate superionic transport, percolating free volume can be leveraged to promote ion hopping through interconnected voids.^{30,31} One definition of free volume is the total volume of a system minus the volume occupied by the molecules.³² Free-volume voids can originate from imperfect chain packing (e.g., packing frustration).^{33–35} The total free volume

and the size distribution of these free-volume voids can be characterized using several experimental techniques such as, positron annihilation lifetime spectroscopy, which probes positron lifetimes in the material,^{36–39} inverse gas chromatography, in which the average void size is inferred from the size of the sorbate molecule,³⁷ and ¹²⁹Xe NMR spectroscopy, in which the ¹²⁹Xe chemical shift relative to a gas-phase reference correlates with the free-volume void size.^{37,40–42}

Generally, three key factors can impart chain packing and associated free volume: chain connectivity, chain semi-flexibility, and monomer structure.⁴³ The connectivity between repeat units restricts their mobility; therefore, longer chains increase the degree of packing frustration.⁴⁴ Additionally, bulky backbones and/or side groups limit chain rearrangement, leading to packing-frustrated polymers and decoupled ion transport,^{43,45} as demonstrated in loosely packed poly (ionic liquids)^{44,46–48} and single-ion-conducting (SIC) polymer blends.²⁰ Apart from free volume-support transport, ion hopping through percolating aggregates is another way to obtain superionic transport. For example, in SIC polymers, both molecular dynamics (MD) simulations and experimental results suggested that superionic conduction is achievable *via* hopping through chain-like aggregates, in which one-dimensional ionic channels (due to the hexagonal morphology) and immobilized anion were key determinants.^{49,50} In general, it is desirable if the SPE contains a continuous network of free volume voids for Li⁺ transport while restricting the motion of bulkier anions to enhance favorable Li⁺ conduction.^{19,51} To this end, understanding the impacts of various parameters (polymer structure and architecture, ion-ion correlation, and ion-polymer interaction; see Fig. 2) on superionic transport can provide important insights into efficient SPE design.

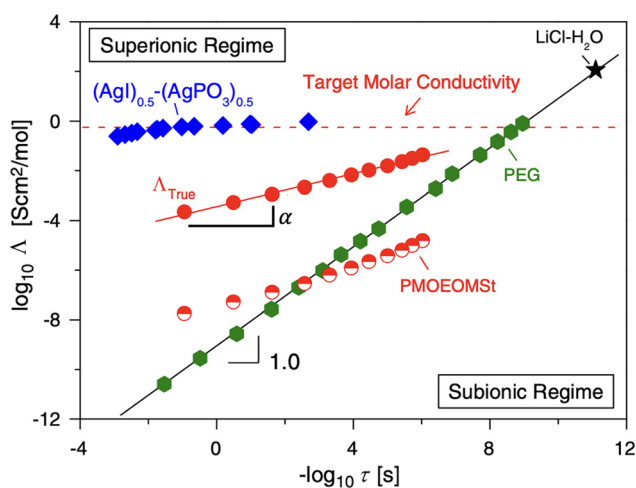


Fig. 1 A typical Walden plot modified for SPEs. Adapted from ref. 23. Copyright 2013 Elsevier B.V.

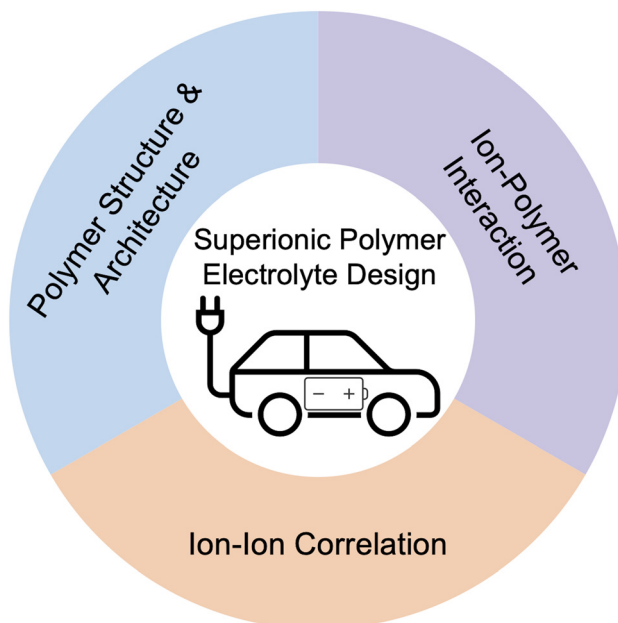


Fig. 2 Key parameters influencing superionic conduction.



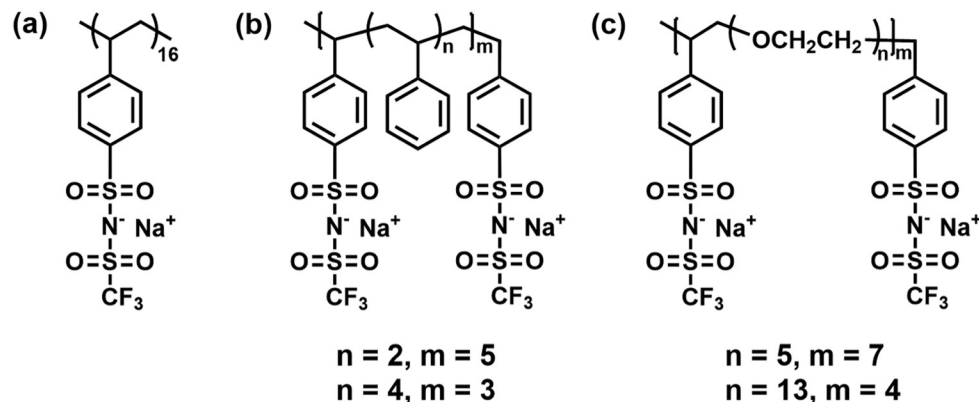


Fig. 3 Chemical structures of the (a) P[STFSINa] homopolymer and copolymers with a (b) polystyrene and (c) polyether spacer. Reprinted from ref. 53. Copyright (2016), with permission from Elsevier.

Polymer structure and architecture

To achieve fast and selective ion transport that is decoupled from polymer segmental dynamics, a pathway is needed through which ions can move without relying on host-polymer relaxation.¹⁶ de Pablo and coworkers demonstrated that in graft polyethers [poly(*oligo*-oxyethylene methyl ether methacrylate) (POEM_x), in which *x* represented the number of ethylene oxide (EO) units in the grafted side chain], two different ion transport events with varying characteristic times were present – a fast intrachain hopping alongside chains and a slow inter-chain hopping between side chains.⁵² Beyond PEO-based materials, similar architecture-dependent transport behavior has been noted in other polymer systems. For example, Chen *et al.* simulated a comb-branched sodium poly[(4-styrenesulfonyl) (trifluoromethanesulfonyl) imide] P[STFSINa] homopolymer and its copolymers with either ether or styrene spacer groups (see Fig. 3) and showed that varying the spacer polarity leads to different ion transport mechanisms.⁵³

The ion hopping mechanism was more dominant in the PSTFSINa homopolymer than in the copolymer systems, due to disruptions of the percolating aggregate network caused by the introduction of polar or non-polar spacers.⁵³ This hopping motion was also noted in Li⁺-based SIC SPEs, in which Kadulkar *et al.* leveraged both experiments and simulations to probe a series of comb-branched SIC copolymers consisting of poly(ethylene glycol) methyl ether acrylate (PEGMEA) with different lithiated anionic groups – acrylic acetate (AA), 2-acrylamido-2-methylpropanesulfonate (AMPS), and methacrylate-propyl (trifluoromethanesulfonyl) imide (MPTFSI).⁵⁴ Copolymers with increasingly bulky anions exhibited a transition in the transport mechanism – from segmental-dynamics-supported motion to hopping motion.⁵⁴ MD simulations revealed that Li⁺ dissociated more rapidly from the larger MPTFSI vs. AMPS and AA.⁵⁴ This dissociation likely led to faster local ion exchange times within the ionic aggregates, maximizing decoupled Li⁺ transport.⁵⁴ Although *t*_{Li⁺} results were not reported, it was suggested that all the systems should

have *t*_{Li⁺}s of ~0.98, determined from the ratio of the molar masses of the anionic repeat unit to Li⁺.^{54–56}

Decoupled transport also can be promoted within the crystalline state of a polymer. Bruce and coworkers demonstrated that in crystalline PEO doped with Li salts (LiPF₆, LiAsF₆, LiSbF₆, or LiClO₄), a co-crystalline phase generated well-defined, cylindrical channels, within which Li⁺ was coordinated by the ether oxygens and underwent hopping-related motion.^{17,57} The anions were located outside of these channels and did not actively participate in Li⁺ coordination (Fig. 4).^{17,57} It has been suggested that ion transport in crystalline regions of PEO is closely related to the molecular alignment of the chains and the presence of the Li⁺ defects within polymer tunnels.^{24,58} Both features collectively promote Li⁺ hopping between sites along the tunnels. The temperature-dependent ionic conductivities followed an Arrhenius relationship.^{24–26} Moreover, the ionic conductivities in semi-crystalline PEO/salt systems were almost two orders of magnitude higher than those of amorphous PEO-like SPEs at similar compositions and molecular weights.^{17,57} Staunton *et al.*



Fig. 4 Schematic of Li⁺ diffusion pathways in PEO₆/LiPF₆, in which PEO₆ indicates that one Li⁺ is coordinated by six ether oxygens. Thin lines represent coordination around Li⁺. Solid blue spheres indicate lithium in the five-coordinate crystallographic site; meshed blue spheres represent lithium in the intermediate four-coordinate site. Representations of carbon atoms are shown in green, and oxygen atoms in red. Adapted with permission from ref. 57. Copyright 2003 American Chemical Society.



found that in semi-crystalline LiPF₆-doped PEO systems, the chain-end chemistry significantly impacted ionic conductivities.²⁹ By replacing the -OCH₃ end group with a bulkier -OC₂H₅ group, a 10× increase in conductivities was realized, despite both systems having similar crystal structures and activation energies²⁹ (estimated from the fitting parameter in eqn (1)).²⁸ The preservation of the crystal structures in the presence of a bulkier -OC₂H₅ end group requires a greater extent of local disorder relative to a -OCH₃ end group.²⁹ This disorder likely increased the number of mobile charge carriers, enhancing the pre-exponential factor in conductivity without altering the energy barrier for ion transport.²⁹

A key challenge in enabling decoupled transport lies in constructing continuous, low-barrier pathways that support efficient ion hopping across different polymer systems. The intrinsic free-volume voids vary in size and are highly dynamic, which can impact transport as they change shape, size distribution, and connectivity. Moreover, ion hopping within ionic aggregates is facilitated when the aggregates form a percolating network, whereas discrete ionic clusters increase transport barriers.

Polymer architecture not only closely correlates with the mode of ion conduction but also influences polymer fragility. Sokolov and co-workers highlighted that the decoupling depends on the system's fragility index (m), *i.e.*, the rate of change of segmental relaxation time (τ) as a function of temperature near T_g [eqn (2)],⁴⁶

$$m \propto \left. \frac{d[\log \tau]}{dT} \right|_{T=T_g} \quad (2)$$

Their work suggested that fragile polymer systems, *i.e.*, those having high energy barriers for intrachain rotations and conformational changes, exhibited significant decoupling of ion transport from polymer segmental relaxation.⁴⁶ In these glassy systems, limited chain flexibility prevents close packing, leaving unstructured free volume that forms percolating networks and facilitates ion hopping.^{16,59} The team studied a series of poly(1-butyl-3-vinylimidazolium)-based poly(ionic liquids) (PILs) with varying pendent groups (Fig. 5a).¹⁸ Decoupled transport was assessed through two routes: (1) PILs

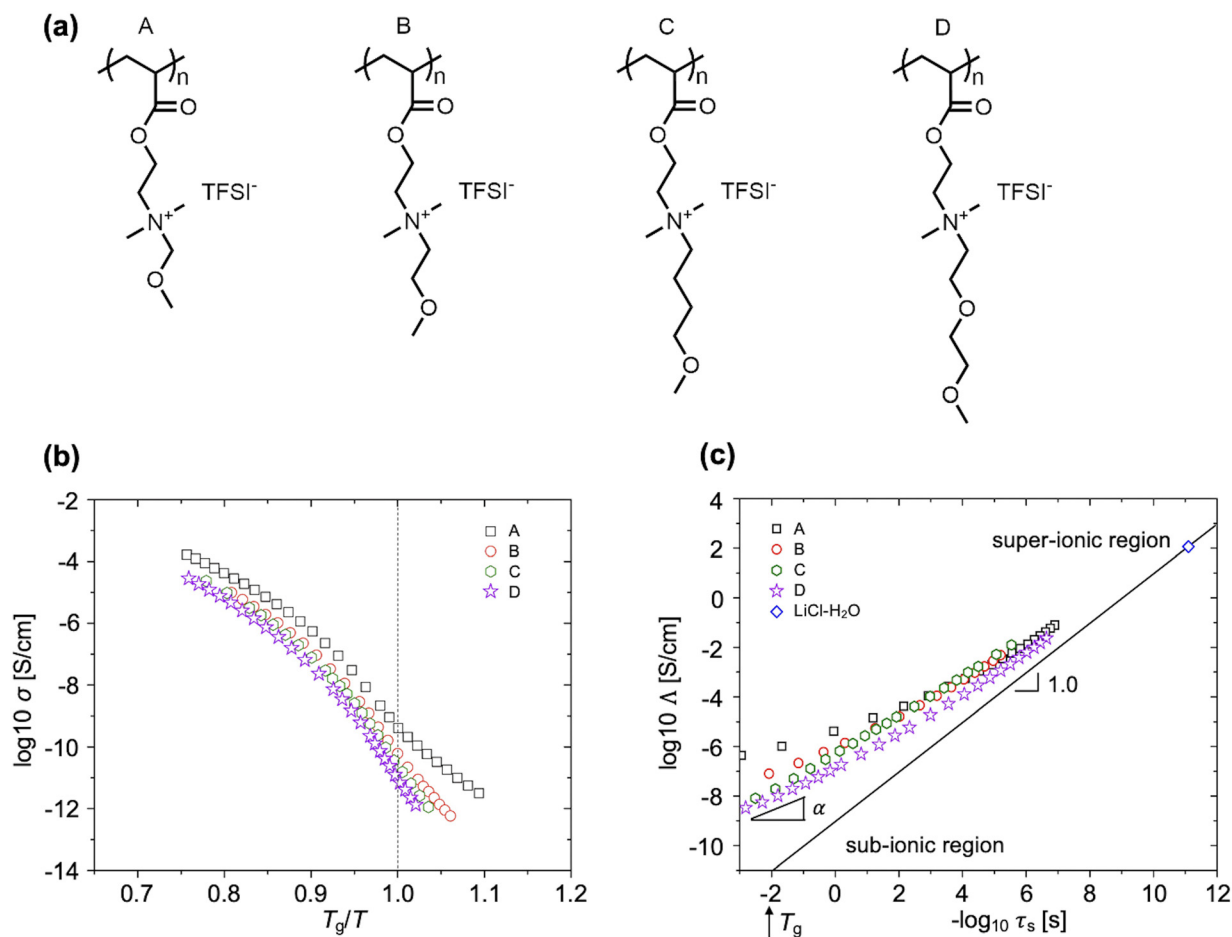


Fig. 5 (a) Chemical structures of PILs with different pendent groups. (b) Ionic conductivity vs. T_g/T . (c) Walden plot (modified for SPEs). The decoupling exponent, $\epsilon = 1 - \alpha$, reflects the degree of decoupling between the ionic conductivity and segmental relaxation in the vicinity of T_g . Adapted with permission from ref. 18. Copyright 2015 American Chemical Society.





Fig. 6 (a) Chemical structures of PILs with different side groups and backbones. (b) Conductivity (top) and free volume (bottom) vs. T_g/T . Adapted with permission ref. 48. Copyright 2017 American Chemical Society.

exhibited conductivities several orders of magnitude higher than $10^{-15} \text{ S cm}^{-1}$ (Fig. 5b) at their T_g s, whereas systems in which ion motion is fully coupled to structural relaxation are expected to have conductivities on the order of $10^{-15} \text{ S cm}^{-1}$ at T_g ,⁶⁰ and (2) the degree of decoupling, ϵ , was calculated as $1 - \alpha$, in which α is the Walden plot slope, and ϵ increased from 0.34 to 0.60 with increasing m of the PILs.¹⁸

The flexibility or rigidity of the polymer backbone and pendent groups also influences both polymer fragility and the extent of decoupling. Wojnarowska *et al.* investigated three aprotic PILs that shared the same ion-counterion pair but differed in side groups and backbone structure.⁴⁸ The side groups included a rigid ethylimidazolium cation, a rigid imidazolium cation connected to an alkyl chain, or a semiflexible imidazolium cation attached to three ethylene glycol units. The backbones were either rigid vinyl-based or flexible siloxane-based (Fig. 6a). Walden plot analysis revealed strong decoupling in the rigid vinyl-based systems but minimal decoupling in the flexible siloxane-based PIL.⁴⁸ Moreover, the flexible siloxane-based PIL had the highest activation energy for transport, as determined by fitting the Arrhenius equation to the experimental data below T_g . In contrast, the PIL with a rigid backbone and rigid side group had the lowest activation energy.⁴⁸ The authors attributed this phenomenon to the reduced free volume in the flexible backbone system (Fig. 6b) that reduced transport pathways.⁴⁸

As an alternative to varying the chemistry and rigidity of polymer side groups and backbones, adjusting molecular weight also can lead to decoupled ion transport. Fan *et al.* investigated the conduction properties of seven PILs with molecular weights ranging from 482 (monomer) to 160 400 g mol^{-1} .⁴⁴ The authors used a modified Walden plot analysis to determine that the system transformed to a strongly decoupled

mechanism as the molecular weight increased.⁴⁴ The authors speculated that more linkages between repeating units in the polymeric cations introduced spatial constraints that hindered efficient chain packing and facilitated decoupling between ion transport and polymer segmental motion.⁴⁴ Similarly, Yang and Epps demonstrated that a binary blend system composed of a semiflexible SIC polymer – poly[lithium sulfonyl(trifluoromethane sulfonyl)imide methacrylate] (PLiMTFSI) – and a flexible, ion-conducting PEO derivative – poly(*oligo*-oxyethylene methyl ether methacrylate) had a shift in ion transport behavior with PLiMTFSI molecular weight.²⁰ As the molecular weight of PLiMTFSI increased from 7 to 52 kg mol^{-1} , the ionic conductivity increased by $\sim 100\times$ due to a transition from transport being closely coupled to the polymer segmental dynamics (Vogel–Tammann–Fulcher [VTF]-like behavior) to more decoupled, Arrhenius-type behavior (Fig. 7). As the molecular weight further increased to 105 kg mol^{-1} , the conduction behavior remained Arrhenius-like, yet the conductivity dropped by almost an order of magnitude, indicating that other factors were also relevant, such as the impact of chain ends.²⁰ A key challenge lies in preserving the interconnectivity of the free volume network that facilitates ion motion. The dynamic and small-scale nature of these voids allows them to change size significantly with minor rearrangements,⁶¹ thereby impacting their size distribution and the corresponding ion transport efficiency.⁶²

Ion–ion correlation and ion–polymer interaction

Understanding ion–ion correlations is crucial in the design of SPEs.⁶³ Cations that are coordinated exclusively by the polar





Fig. 7 Ionic conductivity vs. $1000/T$ for PLiMTFSI – X/POEM blend electrolytes at (a) $r = 5 : 1$, (b) $r = 10 : 1$, (c) $r = 20 : 1$, and (d) $r = 30 : 1$; X represents the number-average molecular weight of the PLiMTFSI, r represents the molar ratio of the ether oxygen in POEM to Li^+ in PLiMTFSI. Solid lines represent the Arrhenius fitting to the conductivity results, whereas dashed lines represent the VTF fitting to the conductivity data. Adapted with permission from ref. 20. Copyright 2024 American Chemical Society.

groups of the polymer hosts are referred to as charge carriers, and their population strongly influences the overall conductivity.⁶⁴ In practical systems, cations may associate with one or more nearby anions to form ion pairs, triplets, or larger clustered species.⁶⁴ The relative populations of these coordination environments reflect a balance between electrostatic interactions among ions and the entropic constraints imposed by the polymer matrix.⁶⁴ Importantly, ion aggregates, particularly electrically neutral species such as ion pairs, do not participate in charge transport and therefore do not enhance conductivity.⁶⁴ The relation between ion diffusion and ionic conduc-

tivity can be well captured by the Nernst–Einstein (NE) equation [eqn (3)],⁶⁵

$$D_{\sigma} = \frac{\sigma k_{\text{B}} T}{n e^2} \quad (3)$$

in which D_{σ} is the charge diffusion coefficient estimated from the experimentally measured conductivity (σ), k_{B} is the Boltzmann constant, T is the absolute temperature, n is the free ion concentration, and e is the charge of the free ion.^{47,65} D_{σ} is usually different from the self-diffusion coefficient of the ions, D_i , which can be obtained from solid-state nuclear mag-



netic resonance spectroscopy.⁴⁷ This phenomenon is expressed by the Haven ratio, H_R [eqn (4)], or the inverse of the Haven ratio, H_R^{-1} [eqn (5)].⁶⁵

$$H_R = \frac{D_i}{D_\sigma} \quad (4)$$

$$H_R^{-1} = \frac{D_\sigma}{D_i} \quad (5)$$

H_R^{-1} is a measure of correlated ionic motion. If ion-ion correlation decreases the conductivity, H_R^{-1} will be below 1,^{47,66} whereas H_R^{-1} is above 1 in many superionic crystals and glasses.^{67,68} A larger-than-one H_R^{-1} also has been reported in PILs doped with a lithium salt, as shown in Fig. 8.⁶⁹

As for ion movement, Ganesan and coworkers simulated ion transport mechanisms in poly(1-butyl-3-vinylimidazolium-hexafluorophosphate) PILs and found that anions move *via* a combination of intra- and inter-molecular ion hopping, which involved the continuous formation and breaking of ion associations.⁷⁰ These associations typically consisted of four tethered cationic monomers bound to two different polymer chains, and the anion mobility was directly linked to the average lifetimes of the ion associations.⁷⁰ The simulation results provided a theoretical foundation for the experimentally reported decoupled ion transport in PILs.^{70–73} Furthermore, Hall and coworkers demonstrated that cation–anion correlations and the associated ion pair residence times decreased as the ion concentration increased using coarse-grained MD simulations.⁷⁴ Similar findings have been reported in experimental work, indicating that less correlated ion motion (cation–anion correlation) was found at higher ion concentrations.^{75,76} Similarly, in precision polyethylene-based SIC ionomers reported by Winey and coworkers, Li^+ travelled along percolat-

ing ion aggregates.⁷⁷ Although percolating pathways were present in these materials, the authors attributed the limited ion mobility and conductivity in these ionomers to the strong association between Li^+ and the carboxylate (COO^-) groups.⁷⁷ In a related work, precision SICs were prepared with a polyethylene backbone and a sulfonated phenyl group pendent on every fifth carbon.⁷⁸ The polymers were fully neutralized by a counterion X^+ (Li^+ , Na^+ , or Cs^+).⁷⁸ MD simulations revealed that the ionic groups nanophase separated from the polymer backbone to form percolating ionic aggregates, and the cations moved between sulfonate groups within these aggregates.⁷⁸

Beyond their direct impact on ion transport, ion–ion correlations and ion–polymer interactions also influence the morphology of the formed aggregates and the associated degree of decoupling. Winey and co-workers also studied a series of precisely segmented polyethylene-like SIC polymers containing sulfonate groups with Li^+ , Na^+ , Cs^+ , or NBU^+ .⁷⁹ In the case of Li^+ -based SIC SPE, a bicontinuous gyroid morphology enabled higher ionic conductivity at a given temperature in comparison to its isotropic layered and hexagonal counterparts.⁷⁹ This enhanced performance was attributed to the three-dimensionally continuous, ion-conduction channels.^{79,80} Additionally, Abbott and Lawson reported the self-assembly of ion aggregates through MD simulations and suggested that the ionic layer structure could be realized in polymers with well-defined side chains.⁸¹ They also showed that strong ionic interactions resulted in more rapid cation movement through aggregates *versus* systems with weaker ionic interactions.⁸¹ This conclusion was experimentally supported by McCloskey and coworkers.⁸²

It is worth noting that both thermodynamic parameters (*e.g.*, temperature, composition) and kinetic factors (*e.g.*, processing history) influence the equilibrium states and the resulting morphologies of ordered materials.^{83–85} In ionomers with monomers neutralized with barium, gallium, zinc, or cobalt cations and a defined number of cations per chain (6 ions per chain), materials often adopt non-equilibrium structures.⁸⁶ The equilibrium state may be approached either by heating the ionomers to elevated temperatures for several days or by aging them at room temperature over several months.⁸⁶ During the transition from non-equilibrium to equilibrium morphologies, polymer chains dissociated and reorganized intramolecular interactions into intermolecular interactions, ultimately forming networked structures, as demonstrated in zinc ionomers.^{86,87} This activated process proceeded more rapidly at higher temperatures.^{86,87} In addition to experimental approaches, theoretical modeling and simulations have provided insight into structure–property relationships in SPEs. Frischknecht and Winey performed microsecond-long, atomistic MD simulations on a series of precise poly(ethylene-co-acrylic acid) ionomers neutralized with lithium.⁸⁸ Their work demonstrated that the ionic aggregates in these systems exhibited a range of morphologies, from isolated clusters to percolated networks.⁸⁸ The aggregates did not achieve a steady-state distribution within the simulation timeframe at a lower temperature (423 K), whereas at a higher temperature of



Fig. 8 Inverse Haven ratio as a function of Li^+ loading. Adapted with permission from ref. 69. Copyright 2022 American Chemical Society.



600 K, the increased mobility of the aggregates allowed them to reorganize and reach steady state after several hundred nanoseconds.⁸⁸ In another example of modeling proton transport within hydrogen-bonded networks, achieving a quantum-mechanical description of covalent and hydrogen-bond breaking and formation requires ion diffusion to be simulated within an equilibrated morphology obtained from density functional theory.⁸⁹ Overall, these examples underscore the complex interplay between structure (morphology), dynamics, and transport in polymer electrolytes and highlight the importance of considering both experimental and computational perspectives when interpreting ion transport behavior.

Conclusions and future directions

Decoupled, superionic conduction is ideal for unlocking next-generation battery technologies that meet increasingly demanding performance and safety requirements. Specifically, branched polymers and packing-frustrated systems with excess free volume can enable ion motion that is faster than the rate of polymer structural relaxation by creating low-energy-barrier conduction pathways. In parallel, SIC polymers with strong ion–ion correlations and tailored ion–polymer interactions can form percolating ionic aggregates to facilitate the formation of continuous transport channels. Beyond SPE systems, gel electrolytes, although outside the scope of this perspective, offer an alternative approach for tuning ion transport.^{90–92} In these systems, the presence of a solvent within a polymer matrix can modulate solvent–cation interactions and alter chain motion, thereby reducing cation–polymer coordination⁹¹ or adjusting the effective width and connectivity of transport channels.⁹² The presence of solvent can increase Li^+ mobility by lowering the energy cost required for Li^+ to dissociate from polymer coordination sites.⁹⁰ For example, quantum chemistry studies have indicated that Li^+ interacts strongly with sulfonate (SO_3^-) groups, which are a functional motif commonly found in anion-containing polymers.^{90,93} These strong $\text{Li}^+ - \text{SO}_3^-$ interactions result in substantial activation barriers for Li^+ dissociation and transport.⁹⁰ The introduction of solvent molecules can partially disrupt these associations, generating transient coordination environments in which Li^+ is preferentially solvated by the solvent molecules with reduced energy barriers, thereby facilitating ion transport.⁹⁰ Together, these emerging design principles offer a promising roadmap for overcoming fundamental transport limitations in SPEs.

Future advances in solid polymer electrolytes will greatly benefit from strategies that enable precise control over polymer sequence and architecture and ion–ion/ion–polymer correlation to unlock rapid and highly selective transport. Sequence-defined polymers, in particular, provide a modular platform for fine-tuning the interconnectivity of transport pathways by precisely controlling the spatial arrangement of ionic and non-ionic segments.^{94–97} Polymer rigidity and flexi-

bility offer additional routes to enhanced ion transport. Polymers with rigid backbones and/or side groups can introduce packing frustration that increases accessible free volume, thereby facilitating ion hopping motion. In contrast, flexible polymer systems can achieve superionic transport by modulating ion concentration to adjust ion–ion correlations, which promotes the formation of favorable ion channels along the polymer matrix. Together, these mechanisms highlight the importance of controlling both polymer conformational freedom and ionic interactions when designing efficient transport networks. Furthermore, achieving an optimal balance between ionic conductivity and cation selectivity requires simultaneous control over polymer chemistry, salt concentration, ion coordination strength, coordination site distribution, phase behavior, and segmental dynamics. Rather than relying solely on iterative electrolyte synthesis and electrochemical testing, the integration of high-throughput synthesis and automated analysis could accelerate the discovery of promising compositions.^{98–104}

In summary, developing a fundamental understanding of the key design parameters that govern superionic conduction in SPEs is essential for advancing high-performance battery technologies. This perspective has highlighted critical insights regarding how polymer characteristics (chain-level architecture and sequence, ion dynamics, and ion–ion correlation environments) impact ion transport behavior. Continued progress in this field will depend on the ability to systematically tailor these features to overcome intrinsic transport limitations. Looking forward, future efforts could prioritize minimizing cation–anion correlations and leveraging labile ion–matrix interactions to promote facile hopping between solvation sites. Several computational studies have demonstrated that introducing a large size asymmetry between cations and anions, or increasing the degree of anion charge delocalization, can effectively enhance ion transport.^{105,106} The integration of machine learning and data-driven modeling approaches will allow quantitative mapping of how phase behavior, ion dynamics, and ionic interaction strength collectively impact ion transport. As data from these efforts accumulate, they can be used to train predictive models to identify composition ranges that maximize ionic conductivity without sacrificing selective cation transport, enabling the efficient design of polymers with superior ion conduction characteristics.

Conflicts of interest

There are no conflicts of interest to declare.

Data availability

No primary research results, software, or code have been included, and no new data were generated or analyzed as part of this perspective.



Acknowledgements

M. Y. and T. H. E. gratefully acknowledge the United States Department of Energy Basic Energy Sciences (DOE BES; DE-SC0014458) for support during the writing of this manuscript.

References

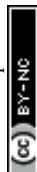
- 1 M. S. Simas, K. Bly, M. A. Arega, F. R. Aponte, T. L. Silva and K. S. Wiebe, Sustainability Effects of Material Demand by Next-Generation Lithium-Ion Battery Technologies: A Global Value Chain Perspective, *Resour., Conserv. Recycl.*, 2025, **219**, 108294.
- 2 P. M. Ketkar, K.-H. Shen, L. M. Hall and T. H. Epps III, Charging Toward Improved Lithium-Ion Polymer Electrolytes: Exploiting Synergistic Experimental and Computational Approaches to Facilitate Materials Design, *Mol. Syst. Des. Eng.*, 2019, **4**(2), 223–238.
- 3 M. A. Morris, H. An, J. L. Lutkenhaus and T. H. Epps III, Harnessing the Power of Plastics: Nanostructured Polymer Systems in Lithium-Ion Batteries, *ACS Energy Lett.*, 2017, **2**(8), 1919–1936.
- 4 M. A. Morris, S. H. Sung, P. M. Ketkar, J. A. Dura, R. C. Nieuwendaal and T. H. Epps III, Enhanced Conductivity via Homopolymer-Rich Pathways in Block Polymer-Blended Electrolytes, *Macromolecules*, 2019, **52**(24), 9682–9692.
- 5 J. Mu, S. Liao, L. Shi, B. Su, F. Xu, Z. Guo, H. Li and F. Wei, Solid-State Polymer Electrolytes in Lithium Batteries: Latest Progress and Perspective, *Polym. Chem.*, 2024, **15**(6), 473–499.
- 6 J. L. Olmedo-Martínez, L. Meabe, R. Riva, G. Guzmán-González, L. Porcarelli, M. Forsyth, A. Mugica, I. Calafel, A. J. Müller, P. Lecomte, C. Jérôme and D. Mecerreyes, Flame Retardant Polyphosphoester Copolymers as Solid Polymer Electrolyte for Lithium Batteries, *Polym. Chem.*, 2021, **12**(23), 3441–3450.
- 7 S. Ren, P. Sang, W. Guo and Y. Fu, Organosulfur Polymer-Based Cathode Materials for Rechargeable Batteries, *Polym. Chem.*, 2022, **13**(40), 5676–5690.
- 8 J. B. Goodenough and K.-S. Park, The Li-Ion Rechargeable Battery: A Perspective, *J. Am. Chem. Soc.*, 2013, **135**(4), 1167–1176.
- 9 K. M. Diederichsen, E. J. McShane and B. D. McCloskey, Promising Routes to a High Li^+ Transference Number Electrolyte for Lithium Ion Batteries, *ACS Energy Lett.*, 2017, **2**(11), 2563–2575.
- 10 S. Manzetti and F. Mariasiu, Electric Vehicle Battery Technologies: From Present State to Future Systems, *Renewable Sustainable Energy Rev.*, 2015, **51**, 1004–1012.
- 11 B. Ravikumar, M. Mynam, S. Repaka and B. Rai, Solvation Shell Dynamics Explains Charge Transport Characteristics of LiB Electrolytes, *J. Mol. Liq.*, 2021, **338**, 116613.
- 12 Y. Choo, D. M. Halat, I. Villaluenga, K. Timachova and N. P. Balsara, Diffusion and Migration in Polymer Electrolytes, *Prog. Polym. Sci.*, 2020, **103**, 101220.
- 13 D. T. Hallinan, S. A. Mullin, G. M. Stone and N. P. Balsara, Lithium Metal Stability in Batteries with Block Copolymer Electrolytes, *J. Electrochem. Soc.*, 2013, **160**(3), A464–A470.
- 14 K. Xu, Navigating the Minefield of Battery Literature, *Commun. Mater.*, 2022, **3**(1), 31.
- 15 J. Min, D. Barpuzary, H. Ham, G.-C. Kang and M. J. Park, Charged Block Copolymers: From Fundamentals to Electromechanical Applications, *Acc. Chem. Res.*, 2021, **54**(21), 4024–4035.
- 16 D. Golodnitsky, E. Strauss, E. Peled and S. Greenbaum, Review—on Order and Disorder in Polymer Electrolytes, *J. Electrochem. Soc.*, 2015, **162**(14), A2551–A2566.
- 17 Z. Gadjourova, Y. G. Andreev, D. P. Tunstall and P. G. Bruce, Ionic Conductivity in Crystalline Polymer Electrolytes, *Nature*, 2001, **412**(6846), 520–523.
- 18 F. Fan, Y. Wang, T. Hong, M. F. Heres, T. Saito and A. P. Sokolov, Ion Conduction in Polymerized Ionic Liquids with Different Pendant Groups, *Macromolecules*, 2015, **48**(13), 4461–4470.
- 19 S. D. Jones, H. Nguyen, P. M. Richardson, Y.-Q. Chen, K. E. Wyckoff, C. J. Hawker, R. J. Clément, G. H. Fredrickson and R. A. Segalman, Design of Polymeric Zwitterionic Solid Electrolytes with Superionic Lithium Transport, *ACS Cent. Sci.*, 2022, **8**(2), 169–175.
- 20 M. Yang and T. H. Epps III, Solid-State, Single-Ion Conducting, Polymer Blend Electrolytes with Enhanced Li^+ Conduction, Electrochemical Stability, and Limiting Current Density, *Chem. Mater.*, 2024, **36**(4), 1855–1869.
- 21 K. I. S. Mongeopa, D. A. Gribble, W. S. Loo, M. Tyagi, S. A. Mullin and N. P. Balsara, Segmental Dynamics Measured by Quasi-Elastic Neutron Scattering and Ion Transport in Chemically Distinct Polymer Electrolytes, *Macromolecules*, 2020, **53**(7), 2406–2411.
- 22 Y. Wang, F. Fan, A. L. Agapov, T. Saito, J. Yang, X. Yu, K. Hong, J. Mays and A. P. Sokolov, Examination of the Fundamental Relation between Ionic Transport and Segmental Relaxation in Polymer Electrolytes, *Polymer*, 2014, **55**(16), 4067–4076.
- 23 Y. Wang, F. Fan, A. L. Agapov, X. Yu, K. Hong, J. Mays and A. P. Sokolov, Design of Superionic Polymers—New Insights from Walden Plot Analysis, *Solid State Ionics*, 2014, **262**, 782–784.
- 24 D. Bresser, S. Lyonnard, C. Iojoiu, L. Picard and S. Passerini, Decoupling Segmental Relaxation and Ionic Conductivity for Lithium-Ion Polymer Electrolytes, *Mol. Syst. Des. Eng.*, 2019, **4**(4), 779–792.
- 25 P. Heitjans and S. Indris, Diffusion and Ionic Conduction in Nanocrystalline Ceramics, *J. Phys.: Condens. Matter*, 2003, **15**(30), R1257–R1289.
- 26 M. A. Ratner, P. Johansson and D. F. Shriver, Polymer Electrolytes: Ionic Transport Mechanisms and Relaxation Coupling, *MRS Bull.*, 2000, **25**(3), 31–37.



- 27 J. Cui, S. Dai, J. He, X. Kong and M. Huang, Solid-State Polymer Electrolytes: Decoupling Lithium-Ion Transport from Relaxation Dynamics of Polymer Chain Segments, *Responsive Mater.*, 2025, e70021.
- 28 M. Petrowsky and R. Frech, Temperature Dependence of Ion Transport: The Compensated Arrhenius Equation, *J. Phys. Chem. B*, 2009, **113**(17), 5996–6000.
- 29 E. Staunton, Y. G. Andreev and P. G. Bruce, Factors Influencing the Conductivity of Crystalline Polymer Electrolytes, *Faraday Discuss.*, 2007, **134**, 143–156.
- 30 S. K. Sharma and J. Mor, Free Volume Mediated Decoupling of Ionic Conduction from Segmental Relaxation Leading to Enhancement in Ionic Conductivity of Polymer Electrolytes at Low Temperatures, *ACS Macro Lett.*, 2024, **13**(9), 1211–1217.
- 31 N. Ramesh and J. L. Duda, A Modified Free-Volume Model: Correlation of Ion-Conduction in Strongly Associating Polymeric Materials, *J. Membr. Sci.*, 2001, **191**(1), 13–30.
- 32 R. P. White and J. E. Lipson, Polymer Free Volume and Its Connection to the Glass Transition, *Macromolecules*, 2016, **49**(11), 3987–4007.
- 33 D. J. Hoffman, S. M. Fica-Contreras and M. D. Fayer, Amorphous Polymer Dynamics and Free Volume Element Size Distributions from Ultrafast IR Spectroscopy, *Proc. Natl. Acad. Sci. U. S. A.*, 2020, **117**(25), 13949–13958.
- 34 M. A. Otmi, F. Willmore and J. Sampath, Structure, Dynamics, and Hydrogen Transport in Amorphous Polymers: An Analysis of the Interplay between Free Volume Element Distribution and Local Segmental Dynamics from Molecular Dynamics Simulations, *Macromolecules*, 2023, **56**(22), 9042–9053.
- 35 M. Galizia, W. S. Chi, Z. P. Smith, T. C. Merkel, R. W. Baker and B. D. Freeman, 50th Anniversary Perspective: Polymers and Mixed Matrix Membranes for Gas and Vapor Separation: A Review and Prospective Opportunities, *Macromolecules*, 2017, **50**(20), 7809–7843.
- 36 J. Mor and S. K. Sharma, Decoupling of Ion-Transport from Polymer Segmental Relaxation and Higher Ionic-Conductivity in Poly(Ethylene Oxide)/Succinonitrile Composite-Based Electrolytes Having Low Lithium Salt Doping, *Phys. Chem. Chem. Phys.*, 2024, **26**(17), 13306–13315.
- 37 Y. P. Yampolskii, Methods for Investigation of the Free Volume in Polymers, *Russ. Chem. Rev.*, 2007, **76**(1), 59–78.
- 38 V. Shantarovich, I. Kevdina, Y. P. Yampolskii and A. Y. Alentiev, Positron Annihilation Lifetime Study of High and Low Free Volume Glassy Polymers: Effects of Free Volume Sizes on the Permeability and Permselectivity, *Macromolecules*, 2000, **33**(20), 7453–7466.
- 39 M. R. Elsharkawy and W. M. Mohammed, Effect of the Electric Field on the Free Volume Investigated from Positron Annihilation Lifetime and Dielectric Properties of Sulfonated PVC/PMMA, *Polym. Adv. Technol.*, 2024, **35**(7), e6519.
- 40 K. S. Han, S. Ko, Y. Shin, E. D. Walter, M. Taufique, W. Kuang and K. L. Simmons, Effects of Short-Chain Branching on Morphology and Free Volume in Polyethylene under Hydrogen Pressurization Studied by ^1H , ^{13}C , and ^{129}Xe NMR, *J. Phys. Chem. B*, 2026, **130**(1), 630–639.
- 41 K. Bartik, P. Choquet, A. Constantinesco, G. Duhamel, J. Fraissard, J.-N. Hyacinthe, J. Jokisaari, E. Locci, T. J. Lowery and M. Luhmer, Xenon NMR as a Probe for Microporous and Mesoporous Solids, Polymers, Liquid Crystals, Solutions, Flames, Proteins, Imaging, *ChemInform*, 2006, **37**(3), 16–34.
- 42 H. Fujiwara, H. Imai and A. Kimura, Proposition of Hyper-Chemical Exchange Saturation Transfer Subtraction Spectroscopy to Detect Very Weak and Broad Signals Hidden under Baseline and Widen Range of Materials Accessed by Hyperpolarized ^{129}Xe NMR, *ChemPhysChem*, 2025, **26**(23), e202500249.
- 43 J. Dudowicz, K. F. Freed and J. F. Douglas, Fragility of Glass-Forming Polymer Liquids, *J. Phys. Chem. B*, 2005, **109**(45), 21350–21356.
- 44 F. Fan, W. Wang, A. P. Holt, H. Feng, D. Uhrig, X. Lu, T. Hong, Y. Wang, N.-G. Kang, J. Mays and A. P. Sokolov, Effect of Molecular Weight on the Ion Transport Mechanism in Polymerized Ionic Liquids, *Macromolecules*, 2016, **49**(12), 4557–4570.
- 45 R. Kumar, M. Goswami, B. G. Sumpster, V. N. Novikov and A. P. Sokolov, Effects of Backbone Rigidity on the Local Structure and Dynamics in Polymer Melts and Glasses, *Phys. Chem. Chem. Phys.*, 2013, **15**(13), 4604–4609.
- 46 A. L. Agapov and A. P. Sokolov, Decoupling Ionic Conductivity from Structural Relaxation: A Way to Solid Polymer Electrolytes?, *Macromolecules*, 2011, **44**(11), 4410–4414.
- 47 V. Bocharova and A. P. Sokolov, Perspectives for Polymer Electrolytes: A View from Fundamentals of Ionic Conductivity, *Macromolecules*, 2020, **53**(11), 4141–4157.
- 48 Z. Wojnarowska, H. Feng, Y. Fu, S. Cheng, B. Carroll, R. Kumar, V. N. Novikov, A. M. Kisliuk, T. Saito, N.-G. Kang, J. W. Mays, A. P. Sokolov and V. Bocharova, Effect of Chain Rigidity on the Decoupling of Ion Motion from Segmental Relaxation in Polymerized Ionic Liquids: Ambient and Elevated Pressure Studies, *Macromolecules*, 2017, **50**(17), 6710–6721.
- 49 K.-J. Lin and J. K. Maranas, Superionic Behavior in Polyethylene-Oxide-Based Single-Ion Conductors, *Phys. Rev. E: Stat., Nonlinear, Soft Matter Phys.*, 2013, **88**(5), 052602.
- 50 J. Liu, L. Yang, P. D. Pickett, B. Park and J. L. Schaefer, Li^+ Transport in Single-Ion Conducting Side-Chain Polymer Electrolytes with Nanoscale Self-Assembly of Ordered Ionic Domains, *Macromolecules*, 2022, **55**(17), 7752–7762.
- 51 D. Dong, A. Choudhary and D. Bedrov, Coupling-Decoupling Transition between Li^+ Transport and Segmental Relaxation in Solid Polymer Electrolytes, *CS Appl. Polym. Mater.*, 2020, **2**(12), 5358–5364.
- 52 C. Deng, M. A. Webb, P. Bennington, D. Sharon, P. F. Nealey, S. N. Patel and J. J. de Pablo, Role of



- Molecular Architecture on Ion Transport in Ethylene Oxide-Based Polymer Electrolytes, *Macromolecules*, 2021, **54**(5), 2266–2276.
- 53 X. Chen, F. Chen, M. S. Liu and M. Forsyth, Polymer Architecture Effect on Sodium Ion Transport in PSTFSI-Based Ionomers: A Molecular Dynamics Study, *Solid State Ionics*, 2016, **288**, 271–276.
- 54 S. Kadulkar, Z. W. Brotherton, A. L. Lynch, G. Pohlman, Z. Zhang, R. Torres, A. Manthiram, N. A. Lynd, T. M. Truskett and V. Ganesan, The Importance of Morphology on Ion Transport in Single-Ion, Comb-Branched Copolymer Electrolytes: Experiments and Simulations, *Macromolecules*, 2023, **56**(7), 2790–2800.
- 55 Z. Zhang, B. K. Wheatle, J. Krajniak, J. R. Keith and V. Ganesan, Ion Mobilities, Transference Numbers, and Inverse Haven Ratios of Polymeric Ionic Liquids, *ACS Macro Lett.*, 2019, **9**(1), 84–89.
- 56 K. D. Fong, J. Self, B. D. McCloskey and K. A. Persson, Onsager Transport Coefficients and Transference Numbers in Polyelectrolyte Solutions and Polymerized Ionic Liquids, *Macromolecules*, 2020, **53**(21), 9503–9512.
- 57 Z. Stoeva, I. Martin-Litas, E. Staunton, Y. G. Andreev and P. G. Bruce, Ionic Conductivity in the Crystalline Polymer Electrolytes PEO₆:LiXf₆, X = P, As, Sb, *J. Am. Chem. Soc.*, 2003, **125**(15), 4619–4626.
- 58 A. M. Christie, S. J. Lilley, E. Staunton, Y. G. Andreev and P. G. Bruce, Increasing the Conductivity of Crystalline Polymer Electrolytes, *Nature*, 2005, **433**(7021), 50–53.
- 59 S. D. Jones, J. Bamford, G. H. Fredrickson and R. A. Segalman, Decoupling Ion Transport and Matrix Dynamics to Make High Performance Solid Polymer Electrolytes, *ACS Polym. Au*, 2022, **2**(6), 430–448.
- 60 C. Angell, Recent Developments in Fast Ion Transport in Glassy and Amorphous Materials, *Solid State Ionics*, 1986, **18**, 72–88.
- 61 S. Misra and W. L. Mattice, Atomistic Models of Amorphous Polybutadienes. 3. Static Free Volume, *Macromolecules*, 1993, **26**(26), 7274–7281.
- 62 D. Rigby and R. J. Roe, Molecular Dynamics Simulation of Polymer Liquid and Glass. 4. Free-Volume Distribution, *Macromolecules*, 1990, **23**(26), 5312–5319.
- 63 K. D. Fong, J. Self, B. D. McCloskey and K. A. Persson, Ion Correlations and Their Impact on Transport in Polymer-Based Electrolytes, *Macromolecules*, 2021, **54**(6), 2575–2591.
- 64 A. Maitra and A. Heuer, Understanding Correlation Effects for Ion Conduction in Polymer Electrolytes, *J. Phys. Chem. B*, 2008, **112**(32), 9641–9651.
- 65 F. Kremer and A. Schönhals, *Broadband Dielectric Spectroscopy*, Springer Science & Business Media, 2002.
- 66 Ø. Gullbrekken and S. Kvalvåg Schnell, Coupled, Ion Transport in Concentrated PEO–LiTFSI Polymer Electrolytes, *New J. Chem.*, 2023, **47**(44), 20344–20357.
- 67 A. Marcolongo and N. Marzari, Ionic Correlations and Failure of Nernst-Einstein Relation in Solid-State Electrolytes, *Phys. Rev. Mater.*, 2017, **1**(2), 025402.
- 68 N. Kuwata, X. Lu, T. Miyazaki, Y. Iwai, T. Tanabe and J. Kawamura, Lithium Diffusion Coefficient in Amorphous Lithium Phosphate Thin Films Measured by Secondary Ion Mass Spectroscopy with Isotope Exchange Methods, *Solid State Ionics*, 2016, **294**, 59–66.
- 69 J. T. Bamford, L. W. Gordon, H. K. Beech, C. J. Hawker, R. J. Clément and R. A. Segalman, Elasticity and Cooperative Ion Motion in a Polymeric Ionic Liquid Loaded with Li Salt, *ACS Macro Lett.*, 2025, **14**(11), 1668–1674.
- 70 S. Mogurampelly, J. R. Keith and V. Ganesan, Mechanisms Underlying Ion Transport in Polymerized Ionic Liquids, *J. Am. Chem. Soc.*, 2017, **139**(28), 9511–9514.
- 71 J. R. Sangoro, C. Iacob, A. Agapov, Y. Wang, S. Berdzinski, H. Rexhausen, V. Strehmel, C. Friedrich, A. Sokolov and F. Kremer, Decoupling of Ionic Conductivity from Structural Dynamics in Polymerized Ionic Liquids, *Soft Matter*, 2014, **10**(20), 3536–3540.
- 72 Z. Wojnarowska, J. Knapik, M. Díaz, A. Ortiz, I. Ortiz and M. Paluch, Conductivity Mechanism in Polymerized Imidazolium-Based Protic Ionic Liquid [H₃SO₃⁺-BVI_m][OTf⁻]: Dielectric Relaxation Studies, *Macromolecules*, 2014, **47**(12), 4056–4065.
- 73 S. Mogurampelly and V. Ganesan, Structure and Mechanisms Underlying Ion Transport in Ternary Polymer Electrolytes Containing Ionic Liquids, *J. Chem. Phys.*, 2017, **146**(7), 074902.
- 74 K.-H. Shen and L. M. Hall, Ion Conductivity and Correlations in Model Salt-Doped Polymers: Effects of Interaction Strength and Concentration, *Macromolecules*, 2020, **53**(10), 3655–3668.
- 75 L. S. Grundy, D. B. Shah, H. Q. Nguyen, K. M. Diederichsen, H. Celik, J. M. DeSimone, B. D. McCloskey and N. P. Balsara, Impact of Frictional Interactions on Conductivity, Diffusion, and Transference Number in Ether- and Perfluoroether-Based Electrolytes, *J. Electrochem. Soc.*, 2020, **167**(12), 120540.
- 76 M. P. Rosenwinkel and M. Schönhoff, Lithium Transference Numbers in PEO/LiTFSI Electrolytes Determined by Electrophoretic NMR, *J. Electrochem. Soc.*, 2019, **166**(10), A1977–A1983.
- 77 A. L. Frischknecht, B. A. Paren, L. R. Middleton, J. P. Koski, J. D. Tarver, M. Tyagi, C. L. Soles and K. I. Winey, Chain and Ion Dynamics in Precise Polyethylene Ionomers, *Macromolecules*, 2019, **52**(20), 7939–7950.
- 78 B. A. Paren, B. A. Thurston, W. J. Neary, A. Kendrick, J. G. Kennemur, M. J. Stevens, A. L. Frischknecht and K. I. Winey, Percolated Ionic Aggregate Morphologies and Decoupled Ion Transport in Precise Sulfonated Polymers Synthesized by Ring-Opening Metathesis Polymerization, *Macromolecules*, 2020, **53**(20), 8960–8973.
- 79 L. Yan, C. Rank, S. Mecking and K. I. Winey, Gyroid and Other Ordered Morphologies in Single-Ion Conducting Polymers and Their Impact on Ion Conductivity, *J. Am. Chem. Soc.*, 2020, **142**(2), 857–866.



- 80 J. Park and K. I. Winey, Double Gyroid Morphologies in Precise Ion-Containing Multiblock Copolymers Synthesized via Step-Growth Polymerization, *JACS Au*, 2022, **2**(8), 1769–1780.
- 81 L. J. Abbott and J. W. Lawson, Effects of Side Chain Length on Ionic Aggregation and Dynamics in Polymer Single-Ion Conductors, *Macromolecules*, 2019, **52**(19), 7456–7467.
- 82 L. J. Abbott, H. G. Buss, J. L. Thelen, B. D. McCloskey and J. W. Lawson, Polyanion Electrolytes with Well-Ordered Ionic Layers in Simulations and Experiment, *Macromolecules*, 2019, **52**(15), 5518–5528.
- 83 L. S. Grundy, S. Fu, M. D. Galluzzo and N. P. Balsara, The Effect of Annealing on the Grain Structure and Ionic Conductivity of Block Copolymer Electrolytes, *Macromolecules*, 2022, **55**(23), 10294–10301.
- 84 H. J. Ryu, D. B. Fortner, S. Lee, R. Ferebee, M. De Graef, K. Misichronis, A. Avgeropoulos and M. R. Bockstaller, Role of Grain Boundary Defects during Grain Coarsening of Lamellar Block Copolymers, *Macromolecules*, 2013, **46**(1), 204–215.
- 85 J. Ren, C. Zhou, X. Chen, M. Dolejsi, G. S. W. Craig, P. A. Rincon Delgadillo, T. Segal-Peretz and P. F. Nealey, Engineering the Kinetics of Directed Self-Assembly of Block Copolymers Toward Fast and Defect-Free Assembly, *ACS Appl. Mater. Interfaces*, 2018, **10**(27), 23414–23423.
- 86 A. Batra, C. Cohen, H. Kim, K. I. Winey, N. Ando and S. M. Gruner, Counterion Effect on the Rheology and Morphology of Tailored Poly (Dimethylsiloxane) Ionomers, *Macromolecules*, 2006, **39**(4), 1630–1638.
- 87 A. Batra, C. Cohen and T. Duncan, Synthesis and Rheology of Tailored Poly (Dimethylsiloxane) Zinc and Sodium Ionomers, *Macromolecules*, 2006, **39**(1), 426–438.
- 88 A. L. Frischknecht and K. I. Winey, The Evolution of Acidic and Ionic Aggregates in Ionomers during Microsecond Simulations, *J. Chem. Phys.*, 2019, **150**(6), 064901.
- 89 Z. Zhu and S. J. Paddison, Perspective: Morphology and Ion Transport in Ion-Containing Polymers from Multiscale Modeling and Simulations, *Front. Chem.*, 2022, **10**, 981508.
- 90 D. L. Vigil, B. T. Ferko, A. Saumer, S. Mecking, M. J. Stevens, K. I. Winey and A. L. Frischknecht, Partial Solvation of Lithium Ions Enhances Conductivity in a Nanophase-Separated Polymer Electrolyte, *Chem. Mater.*, 2024, **36**(19), 9970–9979.
- 91 H. O. Ford, B. Park, J. Jiang, M. E. Seidler and J. L. Schaefer, Enhanced Li^+ Conduction within Single-Ion Conducting Polymer Gel Electrolytes via Reduced Cation–Polymer Interaction, *ACS Mater. Lett.*, 2020, **2**(3), 272–279.
- 92 J. M. Clary, L. Wang, Y. Yan, A. L. Frischknecht and D. Vigil-Fowler, Effect of Stoichiometry and Hydration Level on Water Domain Size and Transport in Poly (Aryl Piperidinium) Alkaline Anion-Exchange Membranes, *J. Membr. Sci.*, 2025, **717**, 123517.
- 93 M. J. Stevens and S. L. B. Rempe, Binding of Li^+ to Negatively Charged and Neutral Ligands in Polymer Electrolytes, *J. Phys. Chem. Lett.*, 2023, **14**(45), 10200–10207.
- 94 S. Han, P. Wen, H. Wang, Y. Zhou, Y. Gu, L. Zhang, Y. Shao-Horn, X. Lin and M. Chen, Sequencing Polymers to Enable Solid-State Lithium Batteries, *Nat. Mater.*, 2023, **22**(12), 1515–1522.
- 95 E. B. Trigg, T. W. Gaines, M. Maréchal, D. E. Moed, P. Rannou, K. B. Wagener, M. J. Stevens and K. I. Winey, Self-Assembled Highly Ordered Acid Layers in Precisely Sulfonated Polyethylene Produce Efficient Proton Transport, *Nat. Mater.*, 2018, **17**(8), 725–731.
- 96 A. Nishimoto, K. Agehara, N. Furuya, T. Watanabe and M. Watanabe, High Ionic Conductivity of Polyether-Based Network Polymer Electrolytes with Hyperbranched Side Chains, *Macromolecules*, 1999, **32**(5), 1541–1548.
- 97 M. W. Schulze, L. D. McIntosh, M. A. Hillmyer and T. P. Lodge, High-Modulus, High-Conductivity Nanostructured Polymer Electrolyte Membranes via Polymerization-Induced Phase Separation, *Nano Lett.*, 2014, **14**(1), 122–126.
- 98 M. A. Stolberg, J. Lopez, S. D. Cawthorn, A. Herzog-Arbeitman, H.-K. Kwon, D. Schweigert, A. Anapolosky, B. D. Storey, J. A. Johnson and Y. Shao-Horn, A Data-Driven Platform for Automated Characterization of Polymer Electrolytes, *Matter*, 2025, **8**(6), 102129.
- 99 P. H. Svensson, P. Yushmanov, A. Tot, L. Kloo, E. Berg and K. Edström, Robotised Screening and Characterisation for Accelerated Discovery of Novel Lithium-Ion Battery Electrolytes: Building a Platform and Proof of Principle Studies, *Chem. Eng. J.*, 2023, **455**, 140955.
- 100 T. Xie, A. France-Lanord, Y. Wang, J. Lopez, M. A. Stolberg, M. Hill, G. M. Leverick, R. Gomez-Bombarelli, J. A. Johnson and Y. Shao-Horn, Accelerating Amorphous Polymer Electrolyte Screening by Learning to Reduce Errors in Molecular Dynamics Simulated Properties, *Nat. Commun.*, 2022, **13**(1), 3415.
- 101 A. Benayad, D. Diddens, A. Heuer, A. N. Krishnamoorthy, M. Maiti, F. L. Cras, M. Legallais, F. Rahmanian, Y. Shin and H. Stein, High-Throughput Experimentation and Computational Freeway Lanes for Accelerated Battery Electrolyte and Interface Development Research, *Adv. Energy Mater.*, 2022, **12**(17), 2102678.
- 102 G. Bradford, J. Lopez, J. Ruza, M. A. Stolberg, R. Osterude, J. A. Johnson, R. Gomez-Bombarelli and Y. Shao-Horn, Chemistry-Informed Machine Learning for Polymer Electrolyte Discovery, *ACS Cent. Sci.*, 2023, **9**(2), 206–216.
- 103 R. Kumar, M. C. Vu, P. Ma and C. V. Amanchukwu, Electrolytics: A Unified Big Data Approach for Electrolyte Design and Discovery, *Chem. Mater.*, 2025, **37**(8), 2720–2734.
- 104 Y. Zhao, R. J. Mulder, S. Houshyar and T. C. Le, A Review on the Application of Molecular Descriptors and Machine Learning in Polymer Design, *Polym. Chem.*, 2023, **14**(29), 3325–3346.



- 105 Y. Cheng, J. Yang, J.-H. Hung, T. K. Patra and D. S. Simmons, Design Rules for Highly Conductive Polymeric Ionic Liquids from Molecular Dynamics Simulations, *Macromolecules*, 2018, **51**(17), 6630–6644.
- 106 N. Molinari, J. P. Mailoa and B. Kozinsky, Effect of Salt Concentration on Ion Clustering and Transport in Polymer Solid Electrolytes: A Molecular Dynamics Study of PEO–LiTFSI, *Chem. Mater.*, 2018, **30**(18), 6298–6306.

